Optimizing PEGylation of TiO_2 Nanocrystals through a Combined Experimental and Computational Study.

Daniele Selli, Massimo Tawfilas, Michele Mauri, Roberto Simonutti, Cristiana Di Valentin[1]

Dipartimento di Scienza dei Materiali, Università di Milano-Bicocca,
via R. Cozzi 55, 20125 Milano, Italy

SUPPORTING INFORMATION

[1] Corresponding author: cristiana.divalentin@unimib.it

S1.1 Experimental Materials And Methods

General Considerations.

Succinic anhydride (95%), potassium carbonate (K_2CO_3), Sodium Sulfate ($NaSO_3$, 99.9%), 4-dimethylaminopyridine (DMAP), triethylamine (TEA), Titanium (IV) butoxide (TB, 97%), oleic acid (OLAC, 90%), oleyl amine (OLAM, 70%), Ammonium hydroxide solution (NH_4OH, 28%), absolute ethanol (≥ 99.8%), hexane (≥ 95%), absolute methanol (>99.9%) dimethylformamide (DMF, ≥ 99.9%), phosphoryl chloride ($POCl_3$ >98%) freshly distilled before reactions. Tetrahydrofuran (THF >99%) dried with sodium wire and benzophenone and distilled before the reactions start. Chloroform ($CHCl_3$), dichloromethane (DCM), diethyl ether and toluene (≥ 99.9) were eventually dried over calcium chloride and distilled over activated molecular sieves. 2-methoxyethanol (98%) and polyethylene oxide monomethyl ether polymers (mPEG) purchased from Sigma Aldrich ($\bar{M}_w$ = 500, 2000, 5000, 10000, 20000 gmol-1) were precipitated twice from ethanol, dried by azeotropic distillation from toluene, and stored in a dry nitrogen atmosphere. All chemicals were purchased from Sigma Aldrich except for nitrosonium tetrafluoroborate ($NOBF_4$, 98%) purchased from Alfa Aesar.

Synthesis of anatase TiO_2 nanocrystals.

In a typical reaction, a mixture of 60 mmol of OLAC, 40 mmol of OLAM and 11.7 mL of absolute ethanol are stirred for 15 minutes, then 10 mmol of TB are added dropwise. The mixture is poured in a 40 mL Teflon beaker and stirred for 15 min before being transferred into a 400 mL Teflon-lined stainless-steel autoclave containing 40 mL of a solution of ethanol and water (96% ethanol). The system is then heated to 180 °C for 18 h. The crude product is then centrifuged, precipitating a white powder constituted by titania crystalline NPs covered by oleic acid whose polar terminal group is bound to the surface. The aliphatic portion of oleic acid allows easy dispersal in hexane, an apolar solvent. The particles are precipitated several times in ethanol to remove excess ligands and eventually dispersed in hexane, chloroform or DCM.

Ligand stripping procedure.

Dispersion of TiO_2 particles in hexane is added to a solution of $NOBF_4$ and DMF. The amount of $NOBF_4$ used for the experiment is calculated starting from the OA content estimated with TGA. The resulting biphasic mixture is stirred to maximize the interface where the ligand exchange takes place. As the ligand is substituted by BF^-_4-, the surface polarity changes and NPs are transferred from the non-polar (hexane) to the (DMF) phase, typically within 60 min. The surface modified NPs are then purified by precipitation with the addition of toluene, that is miscible with DMF, then the precipitated NPs are dispersed in water. In order to increase the hydroxyl groups on the NPs surface and to have a ligand free surface, the as prepared particles are treated with a solution of ammonium hydroxide and stirred for 24 hours at 70°C. After that process the particles are purified by centrifugation with water

till the solution reaches pH 7-9. This process was applied in order to maximize surface chemistry homogeneity.

Table S1. Crystal dimensions derived from XRD calculated at (101) peak, reported with their standard deviation, TEM reported with their standard deviation and DLS measurements in water reported with their PDI. BET Specific surface areas as well as ζ-potential measured in water dispersions are reported with their standard deviation.

Sample	XRD	TEM	DLS	PDI	SSABET	ζ-Potential
	nm	nm	nm		m^2g^{-1}	mV
Anatase	5.9±0.4	7.6±1.1	16	0.191	174±7	-27.8±6.5

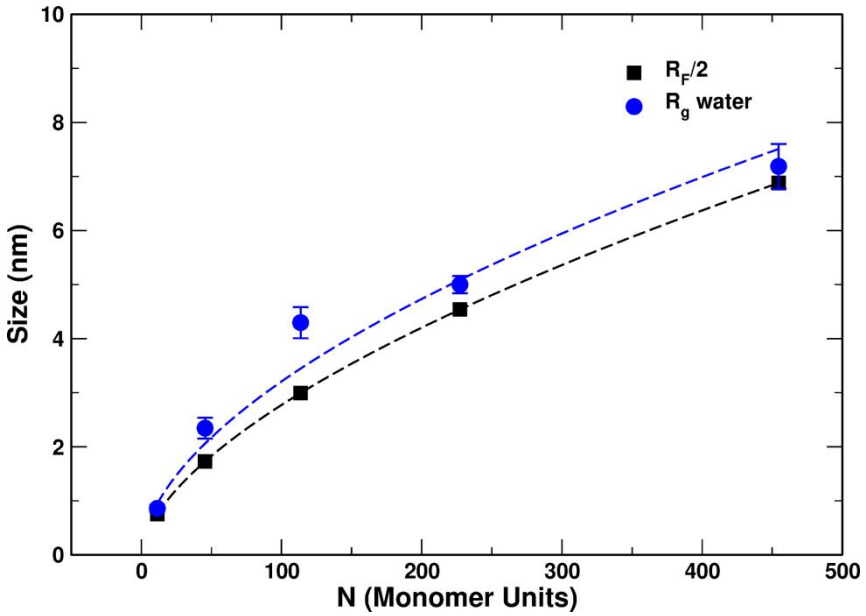

FIGURE S1 Blue circles: plot of radius of gyration measured through DLS analysis as function of the monomer units of the mPEG. The black squares instead represent the calculated Flory radius (R_F) for the same polymer chains. The dashed lines represent the allometric fitting of the experimental points, the fitting function parameters are collected in **Table 2** of the main text.

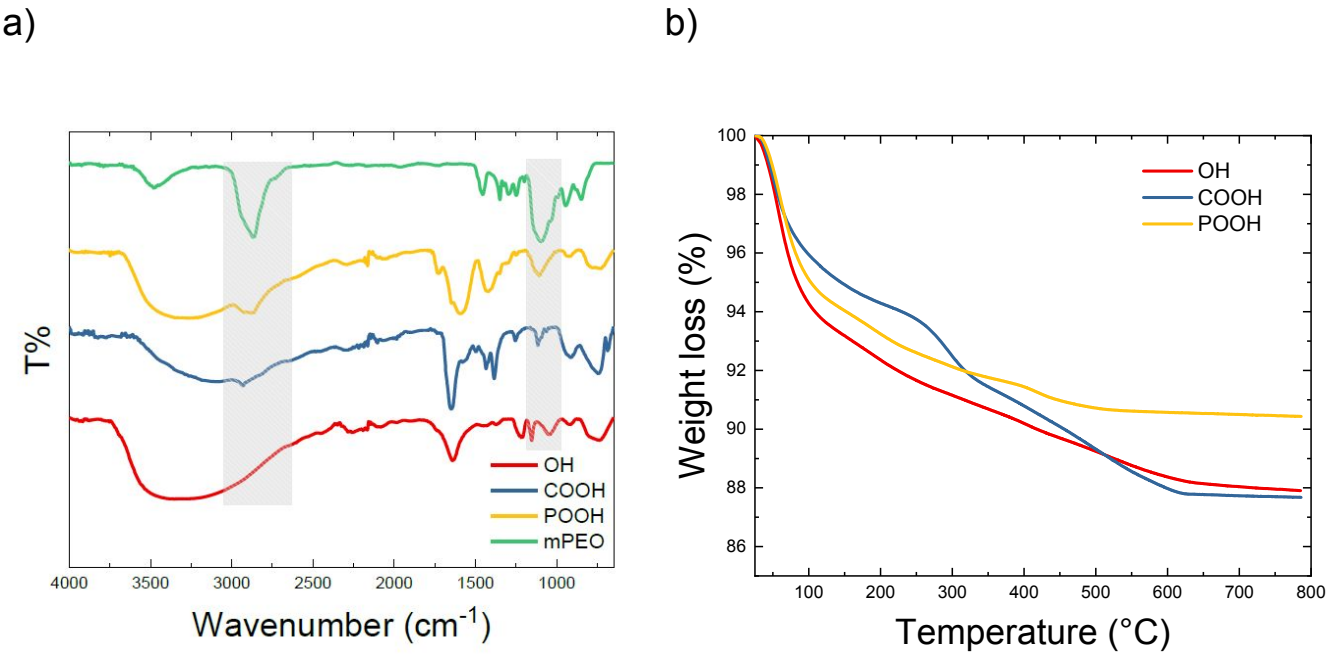

FIGURE S2. a) FTIR spectra plotted as function of the transmission percentage of the grafted anatase NPs in same experimental condition with mPEG ($\overline{M_w}$ 500 gmol^{-1}) in order from top to bottom: mPEG green line, mPEG-PO(OH)$_2$ yellow line, mPEG-COOH blue marine line and mPEG-OH red line. b) Example of TGA of mPEG ($\overline{M_w}$ 500gmol^{-1}) functionalized with POOH yellow line, COOH blue marine line and OH red line grafted on anatase NPs. The weight loss between 150 and 750 °C is used to assess the coverage.

Figure S2 reports the FTIR spectra and the TGA for mPEG$_{500}$@NP samples where the mPEG is terminated with different linkers. In Figure S2a, the green line represents the non-functionalized mPEG chain where the intense vibration peak of the OH terminal group is easily detectable at 3300 cm^{-1}; at 2900 cm^{-1} the peak related to the stretching of the CH_2 groups is detected and at 1100 cm^{-1} the C-O bonds vibration peak. The grey area highlights the region of the spectra where the mPEG peaks are found: it is possible to observe that the peaks appears in the grafted samples (in order from top to bottom: -PO(OH)$_2$ yellow line, -COOH blue line and -OH red line), confirming the presence of the polymer chain on the anatase surface, even if the signal is sometimes hardly detectable.

S2.1 Computational Methods and Models

- *AMBER Force-Fields for $mPEG_{500}$*

To describe the polyethylene $mPEG_{500}$ we used a standard procedure to generate a Generalized Amber Force-Field (GAFF): (i) we optimized the monomer geometry with Gaussian16[1] at the HF/6-31G* level of theory and obtained the charges according to the Merz−Kollman population analysis scheme;[2,3] (ii) we derived the partial atomic charges according to the RESP method[4] utilizing the ANTECHAMBER module.[5] Finally the topology of the whole system was generated with the tLEap module of AMBER16.

- *TiO_2 NP Model*

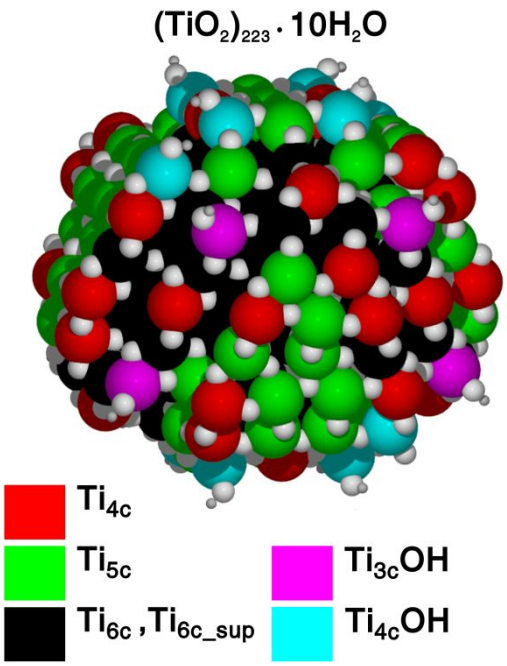

FIGURE S3. Anatase TiO_2 spherical NP model used through this work. The stoichiometry of the system is reported. The color coding indicates the coordination of Ti atoms: red are four-fold coordinated, green are five-fold coordinated, magenta are four-fold coordinated with one position occupied by a –OH group, cyan are five-fold coordinated with one position occupied by a –OH group and black are six-fold coordinate Ti atoms of the bulk and of the surface (i.e. which coordinate at least on O_{2c} atom of the surface). There are 36 Ti_{4c}, 44 Ti_{5c}, 12 Ti_{4c}-OH and 8 Ti_{3c}-OH for a total of 100 Ti atoms which can act as binding sites.

- *Models of $mPEG_{500}$@NP, Water and mPEG Monomers Adsorption*

For the MD simulations of the $mPEG_{500}$@NP systems, different number of methoxy-PEG, H_3CO-$[CH_2CH_2O]_n$-H (with n=11), chains have been attached firstly to the 4-fold coordinated Ti atoms of the curved NP surface and then to the 5-fold coordinated ones keeping the highest possible coverage symmetry (see **Figure S3**). After a first minimization of 50.000 steps to avoid atoms superposition, the O_{PEG}-Ti distance has been kept fixed as well as the position of the NP atoms (corresponding to the DFT(B3LYP) optimized one[6]) exploiting very high Cartesian restraints (5000 kcal mol^{-1} $Å^{-1}$). Using the PACKMOL code[7] the systems have been immersed in 10 nm^3 water boxes with densities of about 1.00 g/cm^3. The number of $mPEG_{500}$ chains used and the relative grafting densities σ are reported in **Table S2**. σ has been calculated considering that the surface of the NP is of 22.2 nm^2.6

Table S2. Number of $mPEG_{500}$ chains attached to NP surface for different grafting densities σ (chain/nm^2).

N. of chains Grafted	Grafting density σ (chain/nm^2)
5	0.225
10	0.440
15	0.676
20	0.901
25	1.126
30	1.351
50	2.252

The molecular (H_2O) or dissociative (OH,H) adsorption of one water molecule on the Ti undercoordinated atoms of the NP surface has been performed, with the DFTB-D3 method, following what we recently published on the same NP functionalized with water.[8] In **Figure S4** all the sites involved have been color coded according to their binding energy strength with water (ΔE_{ads}^{wat} as defined in Section S1.3). In **Table S3** all the ΔE_{ads}^{wat} and binding mode has been reported for all the different kind of sites of the NP surface (see **Figure S4**). When two or three water molecules have been considered, their adsorption mode has been established on the bases of what reported in **Table S3** (e.g. if the two water are on site 16 and 7, they have a dissociative and molecular adsorption mode, respectively). It is important to underline that since the nanoparticle as almost a D_{2d} symmetry the occurrence of each undercoordinated Ti atom, reported in **Table S3**, is more than one: there are 36 Ti_{4c}, 44 Ti_{5c}, 12 Ti_{4c}-OH and 8 Ti_{3c}-OH atoms for a total of 100 Ti which can act as binding sites.

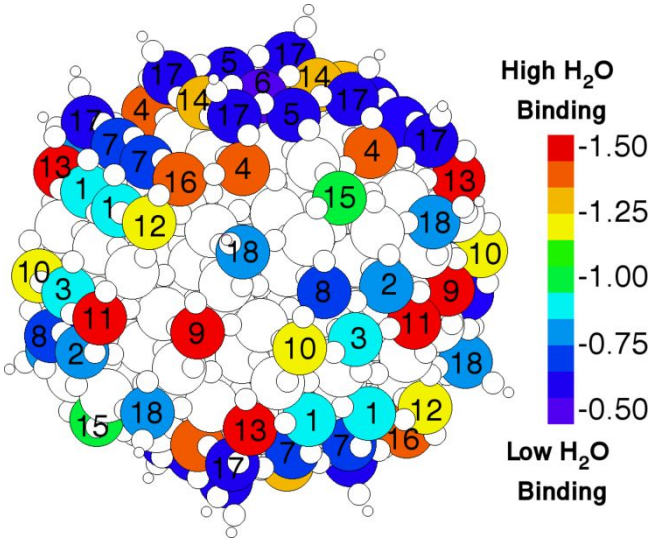

FIGURE S4. Graphical representation of the distribution of binding energies for one water molecularly or dissociatively adsorbed (see **Table S2**) on each undercoordinated Ti site of the NP model in vacuum, as obtained with the DFTB-D3 method.

Table S3. Adsorption energy ΔE_{ads}^{wat} (in eV) and binding mode for single water molecule adsorption on the different Ti sites reported in **Figure S4**.

SITE	Occurrence	Ti-coordination	Binding Mode	ΔE_{ads}^{wat} (in eV)
1	8	5	molecular	-0.89
2	4	5	molecular	-0.80
3	4	5	molecular	-0.90
4	8	5	molecular	-1.37
5	4	5	molecular	-0.59
6	2	5	molecular	-0.53
7	4	5	molecular	-0.72
1	4	4	molecular	-0.76
9	4	4	dissociative	-1.50
10	4	4	dissociative	-1.23
11	4	4	dissociative	-1.54
12	4	4	dissociative	-1.24
13	4	4	dissociative	-1.49
14	4	4	dissociative	-1.28
15	4	4	dissociative	-1.00
16	4	4	dissociative	-1.38
17	12	5 (4-OH)	molecular	-0.78
18	8	4 (3-OH)	molecular	-0.57

a) CH_3-[OCH_2CH_2]-**OH**

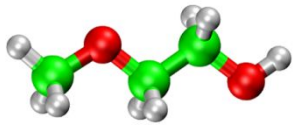

b) CH_3-[OCH_2CH_2]-$O_2C_3H_4$-**COOH**

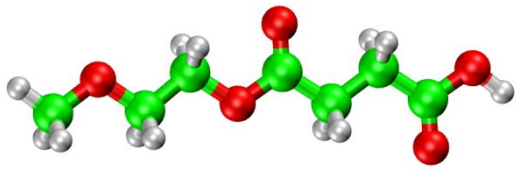

c) CH_3-[OCH_2CH_2]-O-**$PO(OH)_2$**

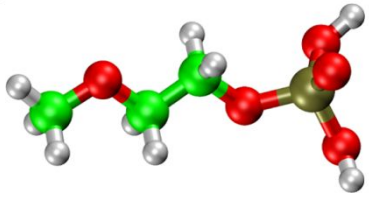

FIGURE S5. Chemical formula and structure for a) –OH (hydroxyl) terminated (2-methoxyethanol), b) –COOH (succinic) terminated (4-(2-Methoxyethoxy)-4-oxobutanoic acid) and c) –$PO(OH)_2$ (phosphate) terminated (2-Methoxyethanol 1-phosphate) mPEG monomers used in this work.

S2.2 MD Analysis Indicators

- *Radius of gyration*

The radius of gyration, R_g^2, has been calculated according to ref [9] as:

$$R_g^2 = \frac{1}{N}\sum_{k=1}^{N}(r_k - r_{mean})^2$$

where r_{mean} is the center of mass of the molecule and r_k the position of each k^{th} heavy atom of the chain. We then report the root-mean-square distance R_g which is averaged over 2000 steps, collected every 2.5 ps for the last 5 ns of the molecular dynamics production run. In the case of the free $mPEG_{500}$ we increased statistic performing three different production runs.

- *End-to-End Distance*

The end-to-end distance, R_{ee}, is the distance between the first and the last heavy atom of the $mPEG_{500}$ chain. Its value is averaged over all the $mPEG_{500}$ chains present in each system and over 2000 steps, collected every 2.5 ps for the last 5 ns of the molecular dynamics production run. In the case of the free $mPEG_{500}$ we increased statistic performing three different production runs.

The calculated *radius of gyration*, R_g and *end-to end distance*, R_{ee} have been compared with other molecular dynamics simulations for PEG of similar size[10,11,12] and experimental data obtained from static light scattering (SLS) measurements in **Table S4**.[13,14]

Table S4. Values of the *radius of gyration*, R_g and *end-to end distance*, R_{ee} (in nm) in water, as calculated in this work (with simulations and experimentally) and from other computational and experimental studies. N refers to the number of monomers present in the PEG chain.

Reference	N	R_g (nm)	R_{ee} (nm)
This work (theory)	11	0.60 ± 0.08	1.43 ± 0.40
This work (experiment)	11	0.90 ± 0.10	-
MD, ref 10	10	0.62 ± 0.09	1.43 ± 0.51
MD, ref 11	9	0.63 ± 0.10	1.51 ± 0.40
MD, ref 12	10	0.62	1.57
[a]Exp, ref 13	11	0.81 ± 0.17	-
[b]Exp ref 14	11	0.62	-

[a] Calculated according to the relation $R_g = 0.0215\ M_w^{(0.583 \pm 0.031)}$
[b] Calculated according to the relation $R_g = 0.0202\ M_w^{0.550}$

- *Mean Distance From the Surface* (MDFS)

It is the distance between the center of mass of each $mPEG_{500}$ polymer and the closest undercoordinated Ti atom of the NP surface. Its value is averaged over all the $mPEG_{500}$ chains present in each system and over 2000 steps, collected every 2.5 ps for the last 5 ns of the molecular dynamics production run (see **Table S5**)

Table S5. Values of the *mean distance from the surface* (MDFS) in nm of $mPEG_{500}$@NP systems immersed in water at different grafting densities σ.

Grafting density σ (chain/nm²)	MDFS (nm)
0.225	1.00 ± 0.11
0.440	1.02 ± 0.06
0.676	0.91 ± 0.06
0.901	0.98 ± 0.03
1.126	1.04 ± 0.04

1.351	0.98 ± 0.03
2.252	1.09 ± 0.01

- *OCCO Dihedral Angles Distribution*

In **Figure S6** we report the dihedral angles distribution of the 10 dihedral angles in the free $mPEG_{500}$ chain in water averaged over 2000 steps, collected every 2.5 ps for the last 5 ns of the molecular dynamics production run. To increase statistic three different production runs have been performed. The distribution has been normalized over the total number of dihedral angles evaluated, i.e. 10 (dihedrals) x 2000 (steps) x 3 (production run) = 60000 angles.

This quantity has been evaluated also for the $mPEG_{500}$@NP systems and thus averaged also over all the $mPEG_{500}$ chains present in each system. In these cases only a single production run have been performed.

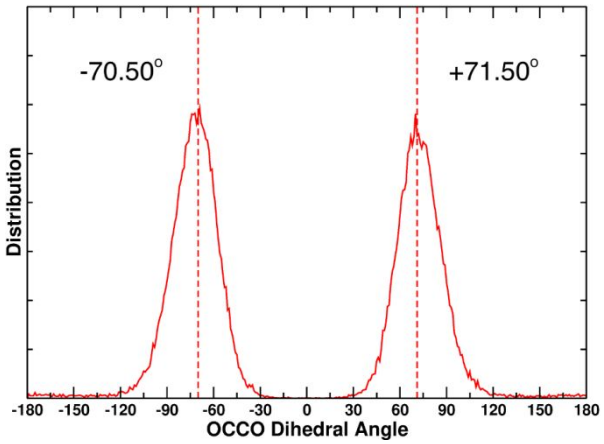

FIGURE S6. Averaged distribution of *OCCO dihedral angles* of the $mPEG_{500}$ chain in water. The majority of the angles have values between ± 30.00° and ± 90.00° corresponding to gauche(-/+) configurations. The two peaks are centered at -70.50° and +71.50°.

- *OCCO Dihedral Angles Index* (DAI)

This index is calculated as follow: (i) in the normalized *OCCO dihedral angles distribution* of each PEG_{500}@NP systems the angles values between ± 90.00° have been removed to highlight the ranges closer to the *trans* (180°) angles; (ii) the resulting function has been integrated between ± 180.00°.

If the free $mPEG_{500}$ and the $mPEG_{500}$@NP chains are similar, the index will be close the average number of *trans* and *cis* dihedrals will be the same in both samples considered. When the index increases the $mPEG_{500}$@NP chains have a larger average number of *trans* and *cis* dihedrals than the free $mPEG_{500}$ indicting more stretched polymers typical of *brush* systems.

- *Number of H-bonds per Monomer*

It is the number of hydrogen bonds between the H atoms of water and the O atoms of the $mPEG_{500}$ chains. Its value is averaged over all the $mPEG_{500}$ chains present in each system and over 2000 steps, collected every 2.5 ps for the last 5 ns of the molecular dynamics production run. In the case of the free $mPEG_{500}$ we increased statistic performing three different production runs. A H-bond is defined when the geometrical criteria of distance $r_{OO} < 3.5$ Å and angle DHA (donor-hydrogen-acceptor) < 150° are encountered.

- *PEG_{500} Volume Fraction:*

The volume fraction, Φ(r), of $mPEG_{500}$ is calculated for the last 100 snapshots of each molecular dynamics simulation of the $mPEG_{500}$@NP systems using spherical layers of 0.09 nm starting from the surface of the NP. For each CH_2 unit and O atom of the PEG we used a volume of 0.02 nm^3, for water of 0.03 nm^3.

S2.3 Monomer Adsorption

- *Adsorption Modes*

Figure S7 reports the different adsorption modes have been considered in this work. In the monodentate and bidentate chelating mode, every monomer occupy one Ti site, in the bidentate bridging two Ti sites and in the tridentate three Ti sites.

For the mPEG-COOH (4-(2-Methoxyethoxy)-4-oxobutanoic acid) there is a case in which the monodentate adsorption occurs without dissociation. For the mPEG-$PO(OH)_2$ (2-Methoxyethanol 1-phosphate) there are some cases, in the monodentate and bidentate bridging adsorption, in which the remaining –OH groups not involved in the covalent bond with the NP donate a proton to the O_{2c} of the surface. All these cases have been highlighted in bold in **Table S7** and **Table S8**, respectively.

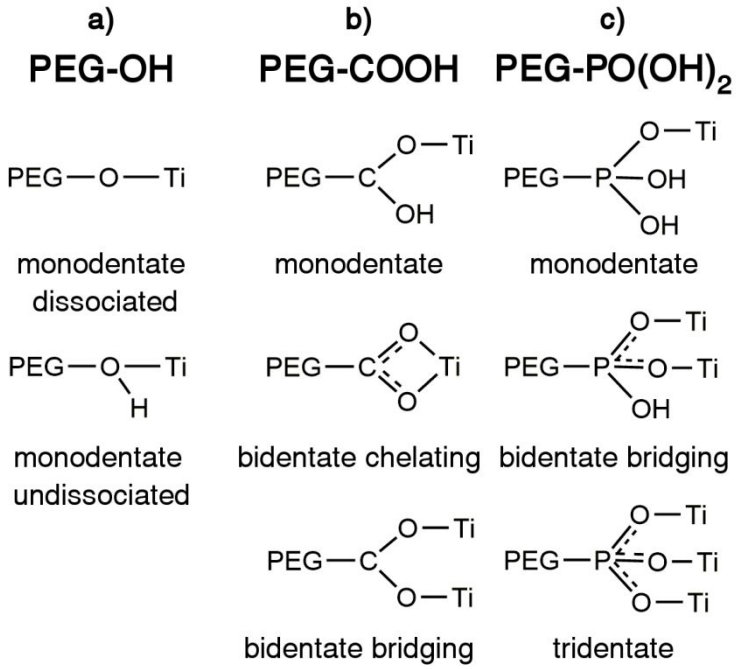

FIGURE S7. Binding modes considered for a) the PEG-OH, b) the PEG-COOH, c) the PEG-$PO(OH)_2$ monomers.

- Adsorption Energies

We have calculated the mPEG monomer adsorption energy (ΔE_{ads}) according to the following equation:

$$\Delta E_{ads} = E_{NP+mon} - E_{NP} - E_{mon}$$

where E_{NP+mon} is the energy of the whole system, E_{NP} is the energy of the bare TiO_2 nanoparticle and E_{mon} is the energy of the mPEG monomer in the gas phase. The water adsorption energy (ΔE_{ads}^{wat}) is:

$$\Delta E_{ads}^{wat} = E_{NP+n_{wat}} - E_{NP} - n_{wat}E_{wat}$$

where $E_{NP+n_{wat}}$ is the energy of the whole system, E_{NP} is the energy of the bare TiO_2 nanoparticle, n_{wat} is the number of water molecule adsorbed on the surface (i.e. $n = 1,2,3$) and E_{wat} is the energy of a single water molecule in the gas phase. To evaluate the loss in energy that we have substituting the water molecule/molecules with the mPEG monomer, we have calculated the competition energy as:

$$\Delta E_{ads}^{comp} = \Delta E_{ads} - \Delta E_{ads}^{wat}$$

For the mPEG-OH (2-methoxyethanol) monomer, values of ΔE_{ads}, ΔE_{ads}^{wat} and ΔE_{ads}^{comp} are reported in **Table S6** together with the type of the Ti atom involved in the binding, the occurrence of that specific Ti and the kind of adsorption of the monodentate mPEG-OH on that site. The binding mode is molecular (if the –OH group remains undissociated), dissociative or "upon condensation". In the last case, a condensation reaction occurs:

$$\text{mPEG-OH + HO-Ti@NP} \rightarrow \text{mPEG-O-Ti@NP + } H_2O$$

where mPEG-OH is the monomer, HO-Ti@NP an undercoordinated Ti site containing an –OH group (Ti_{17} or Ti_{18}), mPEG-O-Ti@NP is the final adduct with the monomer attached to the NP and H_2O is water formed which we adsorb on the closest undercoordinated Ti atom.

Table S6. Binding mode and adsorption energy of the monomer (ΔE_{ads}), water (ΔE_{ads}^{wat}) and competition (ΔE_{ads}^{comp}) for the mPEG-OH on the NP surface.

SITE	Occurrence	Ti-coordination	Binding Mode	ΔE_{ads} (in eV)	ΔE_{ads}^{wat} (in eV)	ΔE_{ads}^{comp} (in eV)
MONODENTATE						
1	8	5	molecular	-1.32	-0.89	-0.43
2	4	5	dissociative	-1.04	-0.80	-0.24
3	4	5	molecular	-1.15	-0.90	-0.25
4	8	5	molecular	-1.72	-1.37	-0.35
5	4	5	dissociative	-1.09	-0.59	-0.42
8	4	4	dissociative	-0.81	-0.76	-0.06
9	4	4	dissociative	-2.12	-1.50	-0.61
11	4	4	dissociative	-2.08	-1.54	-0.53
13	4	4	dissociative	-2.02	-1.49	-0.53
14	4	4	dissociative	-1.78	-1.28	-0.50
15	4	4	dissociative	-1.44	-1.00	-0.44
16	4	4	dissociative	-1.75	-1.38	-0.37
17	12	5 (4-OH)	condensation	-1.98	-1.28	-0.70
18	8	4 (3-OH)	condensation	-1.87	-1.38	-0.49

For the mPEG-COOH monomer, values of ΔE_{ads}, ΔE_{ads}^{wat} and ΔE_{ads}^{comp} are reported in **Table S7** together with the type of the Ti atom (pair of atoms) involved in the binding, the occurrence of that specific Ti (pair of Ti) and the kind of adsorption of the monodentate, bidentate chelated and bidetentate bridging mPEG-COOH on that site (pair of sites).

Table S7. Binding mode and adsorption energy of the monomer (ΔE_{ads}), water (ΔE_{ads}^{wat}) and competition (ΔE_{ads}^{comp}) for the mPEG-COOH on the NP surface. Bold values correspond to the case in which the adsorption occurs in an undissociated mode.

SITE	Occurrence	Ti-coordination	Binding Mode	ΔE_{ads} (in eV)	ΔE_{ads}^{wat} (in eV)	ΔE_{ads}^{comp} (in eV)
MONODENTATE						
1	**8**	**5**	**molecular**	**-1.56**	**-0.89**	**-0.67**
3	4	5	dissociative	-1.28	-0.90	-0.38
4	8	5	dissociative	-2.05	-1.37	-0.68
5	4	5	dissociative	-1.08	-0.59	-0.49
8	4	4	dissociative	-1.16	-0.76	-0.40
9	4	4	dissociative	-2.10	-1.50	-0.60
11	4	4	dissociative	-2.03	-1.54	-0.49
12	4	4	dissociative	-2.08	-1.24	-0.84
14	4	4	dissociative	-1.92	-1.28	-0.64
15	4	4	dissociative	-1.58	-1.00	-0.58
17	12	5 (4-OH)	condensation	-2.39	-1.28	-1.11
BIDENTATE CHELATED						
9	4	4	dissociative	-2.93	-2.40	-0.53
11	4	4	dissociative	-2.73	-2.27	-0.46
12	4	4	dissociative	-2.54	-1.68	-0.86
14	4	4	dissociative	-1.73	-1.14	-0.59
18	8	4 (3-OH)	condensation	-2.57	-2.18	-0.38
BIDENATE BRIDGING						
11-9	4	4-4	diss-diss	-3.09	-3.06	-0.03
10-3	4	4-5	diss-diss	-2.19	-2.00	-0.19
1-12	4	5-4	diss-diss	-2.29	-2.25	-0.04
14-7	4	4-5	diss-diss	-2.30	-2.11	-0.29
2-3	4	5-5	diss-diss	-2.29	-1.55	-0.74
5-6	2	5-5	diss-diss	-1.71	-1.07	-0.64
1-1	4	5-5	diss-diss	-2.45	-1.84	-0.61
12-18	4	4-4 (3-OH)	diss-cond	-2.71	-2.68	-0.03
16-17	4	4-5 (4-OH)	diss-cond	-3.14	-2.78	-0.36

For the mPEG-PO(OH)$_2$ monomer, values of ΔE_{ads}, ΔE_{ads}^{wat} and ΔE_{ads}^{comp} are reported in **Table S8** together with the type of the Ti atom (pair or triplet of atoms) involved in the binding, the occurrence of that specific Ti (pair or triplet of atoms) and the kind of adsorption of the monodentate, bidentate chelated and bidetentate bridging mPEG-PO(OH)$_2$ on that site (pair or triplet of sites).

Table S8 Binding mode and adsorption energy of the monomer (ΔE_{ads}), water (ΔE_{ads}^{wat}) and competition (ΔE_{ads}^{comp}) for the mPEG-PO(OH)$_2$ on the NP surface. Bold values correspond to the case in which –OH groups not involved in the covalent bond with the NP donate a proton to the O_{2c} atoms of the surface.

SITE	Occur.	Ti-coord.	Binding Mode	ΔE_{ads} (in eV)	ΔE_{ads}^{wat} (in eV)	ΔE_{ads}^{comp} (in eV)
MONODENTATE						
1	**8**	**5**	**dissociative**	**-1.87**	**-0.89**	**-0.98**
3	4	5	dissociative	-1.59	-0.90	-0.96
4	8	5	dissociative	-1.97	-1.37	-0.60
5	4	5	dissociative	-1.23	-0.59	-0.64
8	4	4	dissociative	-1.24	-0.76	-0.48
9	4	4	dissociative	-2.42	-1.50	-0.92
11	4	4	dissociative	-1.85	-1.54	-0.31
12	**4**	**4**	**dissociative**	**-2.43**	**-1.24**	**-1.19**
14	4	4	dissociative	-2.58	-1.28	-1.30
15	**4**	**4**	**dissociative**	**-2.02**	**-1.00**	**-1.02**
17	**12**	**5 (4-OH)**	**cond**	**-1.49**	**-1.28**	**-0.21**
BIDENTATE BRIDGING						
9-10	4	4-4	diss-diss	-3.94	-3.13	-0.81
12-16	4	4-4	diss-diss	-2.68	-2.67	-0.01
1-12	**4**	**5-4**	**diss-diss**	**-2.98**	**-2.25**	**-0.73**
4-16	4	5-4	diss-diss	-3.49	-2.78	-0.71
3-10	4	5-4	diss-diss	-2.59	-2.00	-0.59
2-3	4	5-5	diss-diss	-2.47	-1.55	-0.92
5-6	2	5-5	diss-diss	-1.98	-1.07	-0.91
1-1	4	5-5	diss-diss	-2.74	-1.84	-0.90
TRIDENTATE						
1-12-16	4	5-4-4	diss-diss-diss	-1.12	-3.67	+2.55
3-8-10	4	5-4-4	diss-diss-diss	-2.84	-2.73	-0.11
2-3-8	4	5-5-4	diss-diss-diss	-2.99	-2.24	-0.75
7-7-14	4	5-5-4	diss-diss-diss	-3.53	-2.88	-0.65
5-6-14	2	5-5-4	diss-diss-diss	-1.38	-2.42	+1.04
2-3-11	4	5-5-4	diss-diss-diss	-3.57	-2.74	-0.83
12-16-18	4	4-4-4 (3-OH)	diss-diss-cond	-4.00	-3.99	-0.01
7-16-17	4	5-4-5 (4-OH)	diss- diss-cond	-5.12	-3.28	-1.84

- *Full Coverage Design and Adsorption Energy*

As reported in the main text, to obtain a hypothetical full coverage of the NP we followed three steps.

1) We consider the most stable configurations according to their adsorption energy;
2) Each site of the nanoparticle can be occupied only once;
3) We always tried to achieve the maximum coverage possible.

Here we will take the adsorption of the mPEG-COOH in vacuum as an example to show how the full coverage regime is reached and how we evaluated the averaged adsorption energy per molecule. For this example we will always refer to **Table S7**.

I. According to the point 1 the most stable configuration is the one for the Ti pairs 16-17, $\Delta E_{ads} = -3.14$ eV. However, there are only 4 Ti pairs 16-17 on the NP surface, while the Ti_{17} sites are 12 in total. Therefore, we first occupy the 4 Ti pairs 16-17 and then the remaining (because of point 2) 12-4=8 Ti_{17} with the monodentate configuration (adsorption energy of $\Delta E_{ads} = -2.39$ eV). This way also point 3 is satisfied since we occupied 16 Ti atoms: 12 Ti_{17} and 4 Ti_{16} with 12 molecules.

II. The second most stable configuration is the one for the Ti pairs 9-11, $\Delta E_{ads} = -3.09$ eV. However, there are only 4 Ti pairs 9-11 on the NP surface, while singularly the Ti_9 and Ti_{11} sites are 4+4 = 8. Since the sites cannot be occupied twice (point 2) and we want to obtain the highest possible coverage (point 3), we considered the chelated configuration on sites Ti_9 and Ti_{11} with adsorption energy of $\Delta E_{ads} = -2.39$ eV and $\Delta E_{ads} = -2.39$ eV, respectively. This way 8 Ti atoms are occupied with 8 molecules.

III. Following the criteria above we were able to virtually occupy the following Ti single or pairs sites:

SITE	ΔE_{ads} (in eV)	Occurrence
17-16	-3.14	4
9	-2.93	4
11	-2.73	4
18	-2.57	8
12	-2.54	4
1-1	-2.45	4
17	-2.39	8

14-7	-2.30	4
2-3	-2.29	4
4	-2.05	8
5-6	-1.71	2
15	-1.58	4
8	-1.16	4
5	-1.08	2

IV. The ΔE_{ads}^{full} per monomer in the full coverage has been then obtained with:

$$\Delta E_{ads}^{full} = \frac{\sum_i (\Delta E_{ads} \cdot occurence)}{N_{PEG}} = -2.28 \text{ eV}$$

where i run over the different adsorption sites considered in the table above, ΔE_{ads} is their adsorption energy and N_{PEG}=64 is the number of monomers considered to obtain the full coverage. The number of occupied Ti sites is 82.

V. The approximation of this procedure is to consider the PEG monomers completely independent. Furthermore, the statistic of adsorption on the NP surface is not complete. However, we believe that the results are still informative and that in a realistic modeled full coverage there will be only a rigid shift of the ΔE_{ads}^{full} for the different linkers without significant qualitative differences from what we report here.

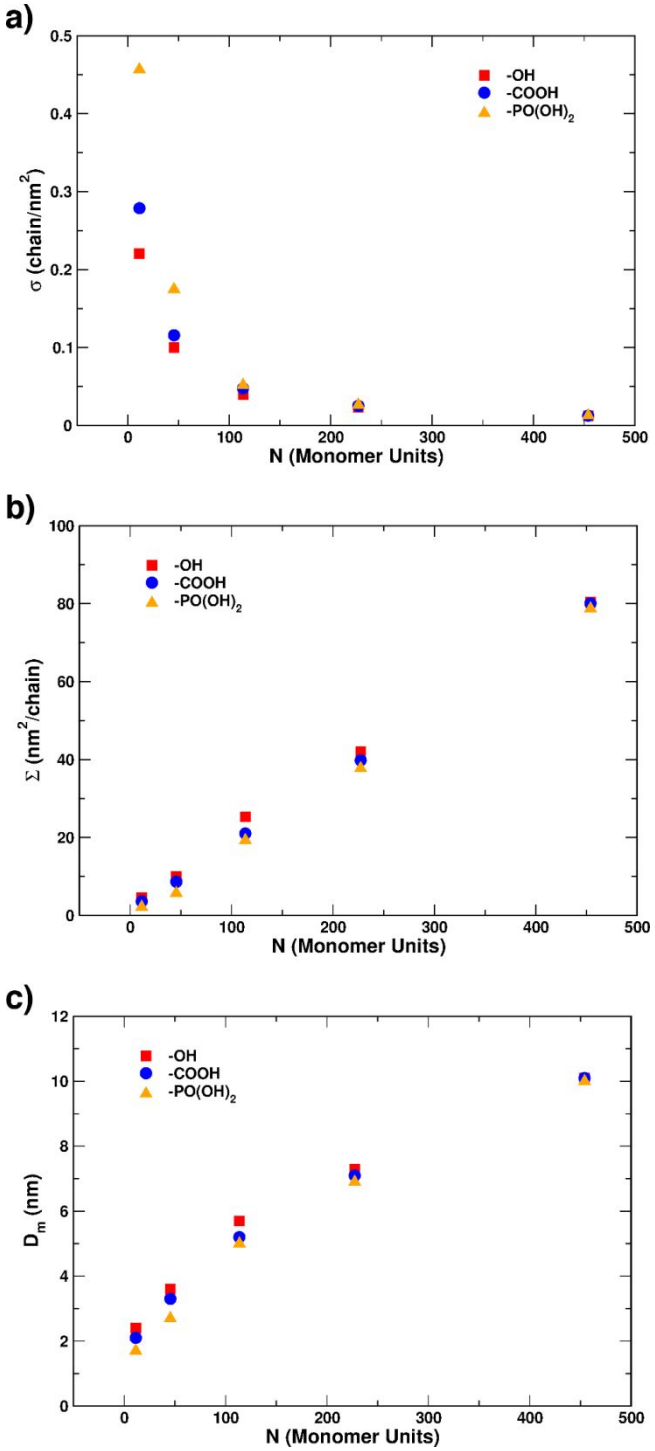

FIGURE S8. a) Grafting density σ, b) footprint Σ and c) mean distance D_m as a function of the number of monomer units in the mPEG chains (see **Table 4** in the main text). Red squares refer to -OH terminated, blue circles to -COOH terminated and yellow triangles to -$PO(OH)_2$ terminated mPEG chains used in the experiments.

REFERENCES

[1] Frisch, M. J.; Trucks, G. W.; Schlegel, H. B.; Scuseria, G. E.; Robb, M. A.; Cheeseman, J. R.; Scalmani, G.; Barone, V.; Petersson, G. A.; Nakatsuji, H.; Li, X.; Caricato, M.; Marenich, A. V.; Bloino, J.; Janesko, B. G.; Gomperts, R.; Mennucci, B.; Hratchian, H. P.; Ortiz, J. V.; Izmaylov, A. F.; Sonnenberg, J. L.; Williams-Young, D.; Ding, F.; Lipparini, F.; Egidi, F.; Goings, J.; Peng, B.; Petrone, A.; Henderson, T.; Ranasinghe, D.; Zakrzewski, V. G.; Gao, J.; Rega, N.; Zheng, G.; Liang, W.; Hada, M.; Ehara, M.; Toyota, K.; Fukuda, R.; Hasegawa, J.; Ishida, M.; Nakajima, T.; Honda, Y.; Kitao, O.; Nakai, H.; Vreven, T.; Throssell, K.; Montgomery, J. A., Jr.; Peralta, J. E.; Ogliaro, F.; Bearpark, M. J.; Heyd, J. J.; Brothers, E. N.; Kudin, K. N.; Staroverov, V. N.; Keith, T. A.; Kobayashi, R.; Normand, J.; Raghavachari, K.; Rendell, A. P.; Burant, J. C.; Iyengar, S. S.; Tomasi, J.; Cossi, M.; Millam, J. M.; Klene, M.; Adamo, C.; Cammi, R.; Ochterski, J. W.; Martin, R. L.; Morokuma, K.; Farkas, O.; Foresman, J. B.; Fox, D. J. Gaussian, Inc., Wallingford CT, 2016.

[2] Besler, B. H.; Merz, K. M.; Kollman, P. A. Atomic Charges Derived from Semiempirical Methods. *J. Comput. Chem.* **1990**, *11*, 431−439.

[3] Singh, U. C.; Kollman, P. A. An Approach to Computing Electrostatic Charges for Molecules. *J. Comput. Chem.* **1984**, *5*, 129− 145.

[4] Bayly, C. I.; Cieplak, P.; Cornell, W. D.; Kollman, P. A. A WellBehaved Electrostatic Potential Based Method Using Charge Restraints for Deriving Atomic Charges: The RESP Model. J. Phys. Chem. 1993, 97, 10269−10280.

[5] Wang, J.; Wang, W.; Kollman, P. A.; Case, D. A. Automatic Atom Type and Bond Type Perception in Molecular Mechanical Calculations. *J. Mol. Graphics Modell.* **2006**, *25*, 247−260.

[6] Selli, D.; Fazio, G.; Di Valentin, C. Modelling Realistic TiO_2 Nanospheres: A Benchmark Study of SCC-DFTB against DFT. *J. Chem. Phys.* **2017**, *147*, 164701.

[7] Martínez, L.; Andrade, R.; Birgin, E. G.; Martinez, J. M. PACKMOL: A Package for Building Initial Configurations for Molecular Dynamics Simulations. *J. Comput. Chem.* **2009**, *30*, 2157−2164.

[8] Fazio, G.; Selli, D.; Ferraro, L.; Seifert, G.; Di Valentin, C. Curved TiO_2 Nanoparticles in Water: How to Model both Short (Chemical) and Long (Physical) Range Interactions. *ACS Appl. Mater. Interfaces*, **2018**, *10*, 29943–29953.

[9] Marshall, F. Radius of Gyration of Polymer Chains. *J. Chem. Phys.* **1962**, *36*, 306-310.

[10] Stanzione, F.; Jayaraman, A. Hybrid Atomistic and Coarse-Grained Molecular Dynamics Simulations of Polyethylene Glycol (PEG) in Explicit Water. *J. Phys. Chem. B* **2016**, *120*, 4160 – 4173.

[11] Lee, H.; Venable, R.M.; MacKerell, A. D. Jr.; Pastor R.W. Molecular Dynamics Studies of Polyethylene Oxide and Polyethylene Glycol: Hydrodynamic Radius and Shape Anisotropy. *Biophys J.* **2008**, *95*, 1590 – 1599.

[12] Prasitnok, K.; Wilson, M. R. A Coarse-Grained Model for Polyethylene Glycol in Bulk Water and at a Water/Air Interface. *Phys. Chem. Chem. Phys.* **2013**, *15*, 17093 – 17104.

[13] Devanand, K.; Selser, J.C. Asymptotic Behavior and Long-Range Interactions in Aqueous Solutions of Poly(ethylene oxide). *Macromolecules* **1991**, *24*, 5943 – 5947.

[14] Kawaguchi, S.; Imait, G.; Suzuki, J.; Miyahara, A.; Kitanoll, T.; Ito, K. Aqueous Solution Properties of Oligo- and Poly(ethylene oxide) by Static Light Scattering and Intrinsic Viscosity. *Polymer* **1997**, *38*, 2885 – 2891.